Sequential Detection for Passive Radar Part 2: the A-C Guard Detector

Tri-Tan Van Cao
Defence Science & Technology (DST) Group
Building 180, DST Group Edinburgh
Adelaide, Australia
tan.cao@dst.defence.gov.au

***Abstract*— Sequential CFAR detection with an alert-confirm (A-C) mechanism is considered for passive coherent location radar. Two sequential detectors are proposed: the A-C direction finding (DF) map detector and the A-C Guard detector. The A-C DF-map detector operates on the DF-map only in its alert step, while its confirm step is performed in the direction of the suspected target's angle-of-arrival. For the A-C Guard detector, the DF-map is approximated by the range-Doppler map obtained by forming the guard channel beam. This Part 2 is devoted to the A-C Guard detector, whereas the A-C DF-map detector is presented in the companion paper Part 1. Monte-Carlo analysis and testing with a real target scenario show that the A-C Guard detector performs comparably with the A-C DF-map detector, while the signal processing load of the A-C Guard is only a fraction of that of the A-C DF-map.**

Keywords*— *Passive coherent location radar; CFAR detection; sequential alert-confirm detector; guard channel.

I. INTRODUCTION

A multi-channel passive coherent location (PCL) radar can perform target detection by taking advantage of a surveillance space which has been illuminated constantly by broadcasting sources such as FM radio, VHF/UHF digital terrestrial television broadcasting signals, and/or communication satellite signals [1]. Within a single coherent processing interval (CPI), a multi-channel PCL radar can completely scan through the whole surveillance space by forming multiple receive beams and then by checking for targets in each cell of the range-Doppler (RD) map obtained at each beam. Consequently, the multi-channel PCL signal processing load is many times heavier than that of an active radar which performs the same surveillance task over a number of CPIs. Such huge signal processing and detection load poses a problem for the real-time capability of a multi-channel PCL system.

In a companion paper [2], the design of a sequential detector using the direction finding (DF) map, namely the alert-confirm (A-C) DF-map detector, has been presented aiming at having real-time capability while keeping the detection loss to a minimum. The aim of this paper is to speed-up the processing time of the A-C DF-map algorithm by investigating the feasibility of replacing the DF-map by the Guard channel RD-map. Formation of the DF-map is summarised in the Appendix. As will be made clear later, the Guard RD-map is much more simple to form than the DF-map.

The rationale behind the use of the Guard RD-map is as follows. A common approach to the design of a sequential detector is to perform the alert detection in a coarse resolution setting while performing the confirm detection in a fine resolution setting [3]. For PCL radar, a coarse resolution setting can be realised by forming receive beams with a large azimuth beam-width and/or forming RD-maps with coarse range, Doppler resolutions. This gives a lower number of cells to be checked, allowing a very high (alert) false alarm rate per CPI to be set. This in turn helps to reduce the processing time of the alert step while letting targets with small SNR to pass through to the confirm step. A straight-forward application of this coarse-fine design methodology is to replace the DF-map in the alert step of the A-C DF-map detector with an RD-map obtained from the formation of a receive beam which has a very large azimuth beamwidth. A receive beam which can give the whole 360° surveillance coverage like that of the DF-map is the Guard channel beam.

As illustrated in Fig. 1, the Guard channel beam has uniform gain in all directions, whereas a directional beam has its gain focusing on a particular direction of interest. Conventionally, the Guard channel beam is used for side-lobe blanking in order to distinguish main-lobe targets from side-lobe hits [4].

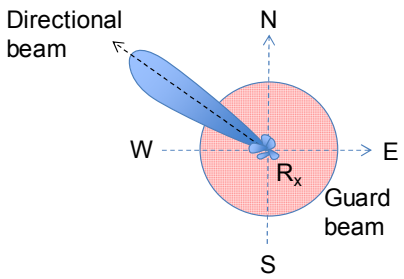

Fig. 1 Illustration of Guard channel beam versus directional beam. Rx: receiver; N: (true) North; E: east; S: South; W: west.

Unlike the DF-map in which each resolution cell contains AoA information (see the Appendix), a target's AoA cannot be deduced from a detection in the Guard RD-map. However, there are two similarities between those two maps:

- Two adjacent cells, either in the DF-map or in the Guard RD-map, may contain two target-like returns from two different directions. This means that a target

in one direction has to compete with targets/clutter in all directions if detection is performed on those two maps.

- For the multi-channel ring array antenna configuration under consideration in this paper, it is observed that the range profiles of the DF-map and of the Guard RD-map are not only statistically similar, but they are also highly correlated. To demonstrate this point, the time-delay profiles at the same Doppler index, one from the DF-map and one from the Guard RD-map, are shown in Fig. 2 (top). A zoom-in is performed at the location where a target-like signal is present, as shown in Fig. 2 (middle). It is evident that those two range profiles almost superimpose on each other. It is also observed that the empirical cumulative density functions (CDFs) of those range profiles fit nicely on each other (Fig.2, bottom).

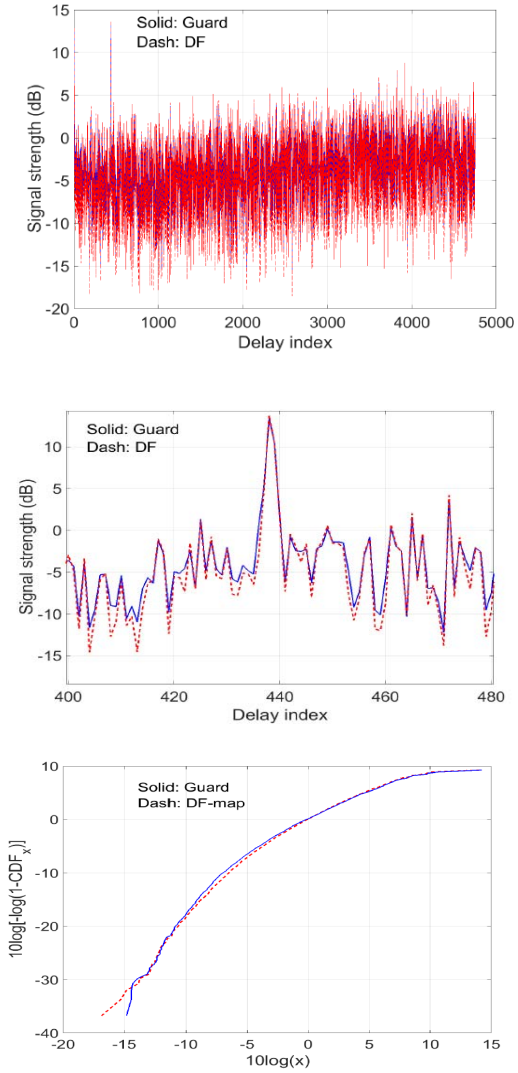

Fig. 2 The range profiles of the Guard RD-map and the DF-map. Top: whole range profile; middle: a zoomed-in section containing a target-like signal; bottom: empirical CDFs of the two range profiles.

Those similarities suggest that the Guard RD-map can be used to replace the DF-map for target detection. Once a target is detected at a location in the Guard RD-map, its AoA can be estimated using the same DF technique used to form the DF-map. The benefit of using the Guard RD-map is that the formation of the DF-map is not required, which means the generation of a data cube consisting of a huge amount of samples as explained in the Appendix can be avoided.

The paper is organized as follows. The new A-C Guard detection scheme is presented in Section II, followed by the analysis of its signal processing and detection loads in Section III. Computation of false alarm probability and detection probability is presented in Sections IV and V, respectively. Performance of the A-C Guard detector is tested using a real target scenario in Section VI, while the discussion and future work are given in Section VII.

II. THE A-C GUARD DETECTION SCHEME

Consider an M-channel PCL receiver in which each antenna element (or channel) is a dipole antenna shown in Fig. 3 (bottom). The cross-correlation and Doppler processing procedure performed at M dipole elements gives M elementary RD-maps which are ready for beamforming [5]. In the far field, each dipole receiver has equal gain in all azimuth directions (omnidirectional) as shown in Fig. 3 (top) [6]. The RD-map of the Guard beam having omnidirectional gain can then be obtained by taking the squared-law of any one of those M elementary RD-maps. To take advantage of the non-coherent integration gain, the Guard channel RD-map can be formed as the non-coherent summation of all M elementary RD-maps. In other words, the Guard channel RD-map, denoted as $\mathbf{G}$, can be formed as:

$$\mathbf{G} = |\mathbf{X}_1|^2 + |\mathbf{X}_2|^2 + \ldots + |\mathbf{X}_M|^2 \quad (1)$$

where $\mathbf{X}_1, \ldots, \mathbf{X}_M$ are M elementary RD-maps. In principle, the Guard channel RD-map can also be formed as a weighted non-coherent summation of those M elementary RD-maps [7].

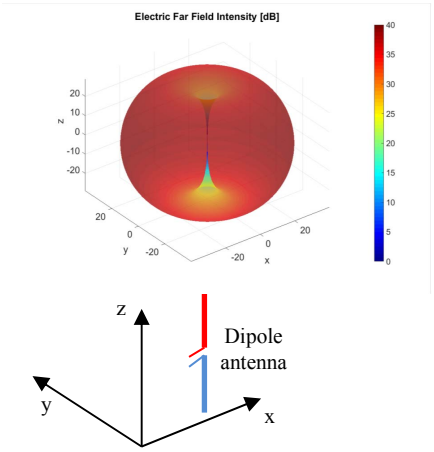

Fig. 3 Dipole antenna. Bottom: dipole orientation; top: dipole omnidirectional far field intensity.

The A-C Guard detector is proposed in Fig. 4 (right). After the formation of M elementary RD-maps at M channels, a target presence/absence decision is made in two steps:

- Alert: the Guard RD-map is formed and each of its cells is checked for the suspicion of a target using the sliding window cell-averaging (CA) technique as follows [8]. Let x be the signal strength in the cell-under-test (CUT). L_1 cells around the CUT are selected to form the set of reference cells $\{x_1,\ldots,x_{L1}\}$. A number of gap cells in the immediate neighbourhood of the CUT are excluded. A target suspicion is declared at the CUT if:

$$x > T_1\mu_1 \tag{2}$$

  Otherwise, target absence is declared. In (2), T_1 is a threshold multiplier constant whose value is determined by the alert false alarm rate F_1; and μ_1 is the interference estimate (the mean of L_1 reference cells).

- Confirm: each Guard RD-map cell that passes the alert test is then checked for target presence/absence. (i) Estimate the AoA of the suspected target in the CUT using the DF algorithm presented in [5]. (ii) Perform beamforming in the estimated AoA to generate the sample z in the CUT and L_2 reference samples $\{z_1,\ldots,z_{L2}\}$. A target is declared present in the CUT if:

$$z > T_2\mu_2 \tag{3}$$

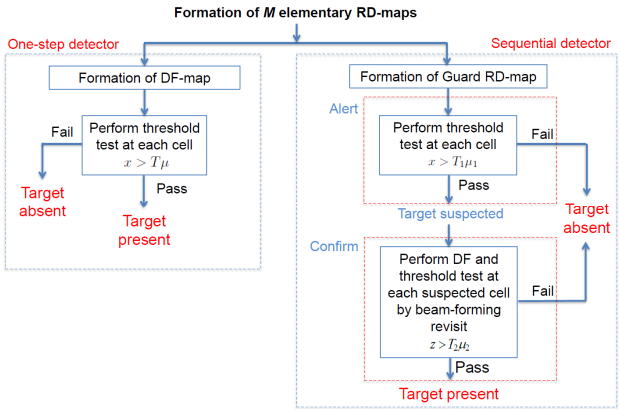

Fig. 4 Sequential A-C Guard detector versus one-step detector.

  Otherwise, target absence is declared. In (3), μ_2 is the interference estimate (the mean of L_2 reference cells); T_2 is a constant determined by the combined alert-confirm false alarm F.

Remark. The order of the tests, (2) then (3), is important. That means conditional probability is required for computing the false alarm and detection probabilities of the sequential detector. This is different from the set of two-stage detectors discussed in [9] where the order of the two tests is not significant. For the sequential detection technique discussed in [3], the confirm test is performed in the next CPI once the alert test has been passed in the current CPI. In this paper, for simplicity, the same CPI is used for both tests (2) and (3).

III. Signal Processing Load

In terms of the signal processing and detection loads, since the A-C DF-map detector is approximately the same as the one-step detector shown in Fig.4 (left) [2], the A-C Guard detector is now compared with the one-step detector.

For the one-step detector in Fig.4 (left), a sliding window CA detector is performed at each cell of the DF-map. As shown in the Appendix, the formation of the DF-map requires the generation of a data cube consisting of KN samples, where K is the number of surveillance angles and N is the number of cells in the DF-map. Note that the DF-map and the Guard RD-map have the same size.

For the A-C Guard detector, since the DF-map is replaced by the Guard RD-map in the alert step, the generation of the data cube consisting of KN samples is not required. In the confirm step, the number of data samples generated for direction finding is $S_1 = KNF_1$, that means, the number of resolution angles (K) times the number of CUTs surviving the alert test (NF_1). The number of data samples generated for the CA threshold test is $S_2 = NF_1L_2$. The total number of data samples generated in the confirm step is then: $S = S_1+S_2 = NF_1(K+L_2)$. The signal processing load ratio A-C-Guard-detector to one-step-detector is then $\rho_1=S/(KN)=F_1[1+(L_2/K)]$.

The number of threshold tests performed by the one-step detector is N (which is the number of cells in the DF-map), while that performed by the A-C Guard detector is $N+NF_1=N(1+F_1)$ (that means, N tests in the alert step and NF_1 tests in the confirm step). The ratio of number of threshold tests, A-C Guard to one-step, is then $\rho_2=N(1+F_1)/N=1+F_1$.

Given typical values F_1= 0.05, L_2=40 reference samples, and K=300 surveillance angles, then $\rho_1\approx0.057$ and $\rho_2=1.05$. In summary, compared with the one-step and the A-C DF-map detectors, the A-C Guard detector's signal processing load is only 6 % while its detection load is approximately the same.

IV. Probability of False Alarm

From (2) and (3), the sequential detector's false alarm is:

$$F=\text{Prob}[x > T_1\mu_1 \mid \text{H}_0]\times\text{Prob}[z > T_2\mu_2 \mid \text{H}_0]|_{\text{alert}}=F_1\times F_2 \tag{4}$$

where H_0 denotes the hypothesis of target absence; and "$|_{\text{alert}}$" denotes a probability conditioned on the event that the alert test has been passed. Since the Guard RD-map has similar statistics as that of the DF-map, from the companion paper [2] the threshold multipliers T_1 in (2) and T_2 in (3) are computed as follows given F_1 and F (for simplicity, let $L_1=L_2=L$):

$$T_1 = [(3F_1)^{-(1/L)} - 1]\,L \tag{5}$$

$$T_2 = [F^{-(1/L)} - 1]\,L \tag{6}$$

Note that (6) is the same as the closed-form formula obtained by applying a CA-CFAR detector on exponentially distributed background [8].

V. PROBABILITY OF DETECTION

The detection probability of the sequential detector is obtained from (4) where hypothesis H_0 is replaced by H_1:

$$P_d = \text{Prob}[x > T_1\mu_1 \mid H_1]\times\text{Prob}[z > T_2\mu_2 \mid H_1]|_{\text{alert}} \qquad (7)$$

where H_1 denotes the hypothesis of target presence. Hypothesis H_1 is realized by injecting artificial targets into experimental data as follows. The 360° surveillance space is divided into eight equal subsectors numbered from 1 to 8 as shown in Fig. 5 (top). The receiver is located at the origin, while the transmitter is located at point Tx which is 164° clock-wise with respect to true North.

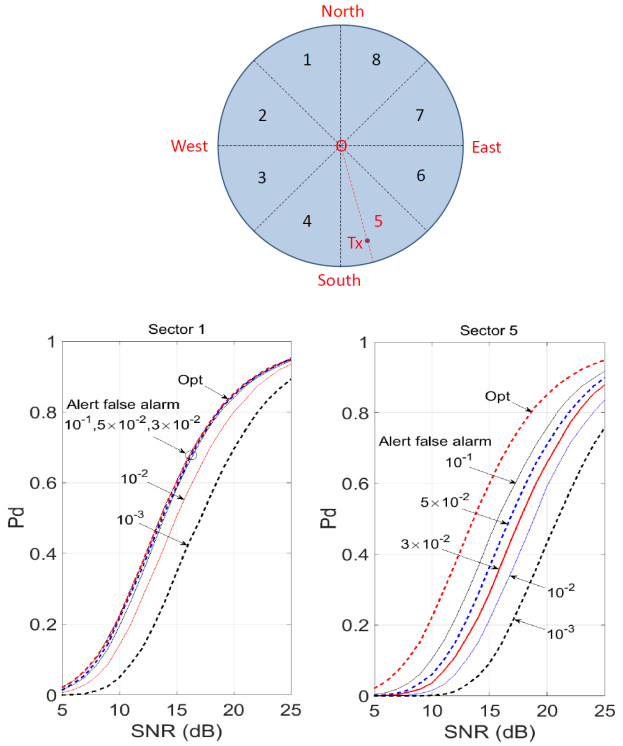

Fig. 5 Detection performance of the A-C Guard detector at overall false alarm rate F=10^{-6}. "Opt": optimal detector.

For the experimental data in use, the receiver parameters are summarised in Table 1, while the transmitter is a Digital Video Broadcast - Terrestrial (DVB-T) with carrier frequency 184.5 MHz and 7 MHz bandwidth.

TABLE I. SUMMARY OF RECEIVER PARAMETERS

Surveillance Elements	**7**
Reference Elements	1
Surveillance Array Configuration	Ring
Surveillance Type	Dipole
Coherence Processing Interval	0.5 s
Frequency Band	171 – 220 MHz

P_d in each sector is estimated by inserting Swerling-1 targets [8] into experimental data with the target's AoA randomly distributed within that sector. The target's signal-to-noise ratio (SNR) is defined as the SNR obtained after beamforming in the direction of the injected target's AoA. Monte-Carlo simulation with 10^4 trials is used for each P_d estimate.

With L_1=L_2=40 and an overall false alarm rate F=10^{-6}, the detection curves of the A-C Guard detector are shown in Fig. 5 (bottom) for different settings of the alert false alarm rate F_1. It is found that the detection performance is best in Sector 1 facing 180° away from the transmitter (Fig. 5, bottom-left) and is worst in Sector 5 facing directly to the transmitter (Fig. 5, bottom-right). This may be due to the strong interference caused by the line-of-sight reference signal. It is observed that the A-C Guard detector performs better with a higher alert false alarm rate. For target detection in Sector 1, Fig.5 (bottom-left), the CFAR loss with respect the optimal curve "Opt" (obtained by applying a sliding-window CA detector on exponentially distributed background) is less than 0.5 dB for F_1> 0.03. A reasonable choice for the alert false alarm rate is then between 0.05 and 0.1. In Fig. 6, detection performance of the A-C Guard detector is compared with that of the A-C DF-map detector (presented in the companion paper [2]). It is evident that in order to achieve approximately the same CFAR loss (with respect to the optimal curve) in both Sector 1 (the best performance) and Sector 5 (the worst performance), the alert false alarm rate of the A-C Guard detector should be set around five times higher than that of the A-C DF-map detector.

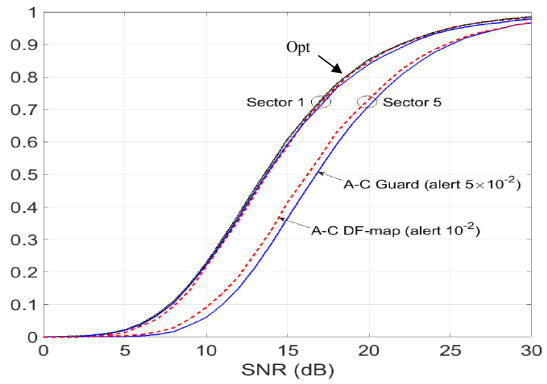

Fig. 6 A-C Guard versus A-C DF-map at overall false alarm rate F=10^{-6}. Dash: A-C DF-map; solid: A-C Guard; "Opt": optimal detector.

VI. DETECTION SCENARIO

Performance of the A-C Guard detector is now examined using data collected by a PCL radar built by the Defence Science & Technology (DST) Group. The receiver has a 7-element ring array and a dedicated reference antenna for line-of-sight signal reception. A total of 300 azimuth-elevation hypotheses are considered, covering 360° azimuth and two layers of elevation. Receiver parameters are shown in Table 1. The reference signal is received from a DVB-T source which transmits at frequency 184.5 MHz with a 7 MHz bandwidth.

The same data file used in [2] is employed here for ease of comparison. Target ground truth scenario is shown in Fig. 7. The receiver is located at the origin (0,0) and is marked as Rx, while the transmitter is 30 km south-east of the receiver and is

marked as Tx (164^O clock-wise from the true north). There is one Boeing 717 aircraft (labelled as B717); three Diamond D40 aircraft DA40(1), DA40(2), and DA40(3); one Diamond D42 aircraft labelled as DA42; and one Fokker F100 labelled as F100. The ground truth of those targets is shown as circles with arrows indicating their heading directions.

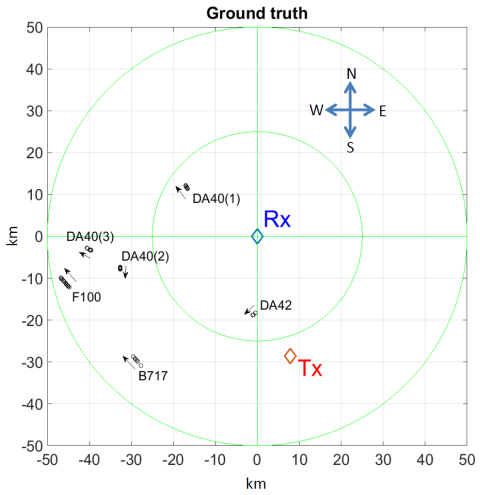

Fig. 7 The ground truth of target scenario.

Parameters of the two detectors are $F=10^{-6}$, $L_1=L_2=40$, and $F_1=10^{-2}$. For both detectors, 5 gap cells on each side of the CUT are used. The data set is processed with a CPI length of 0.5 seconds, giving a total of 44 CPIs.

Target detection versus ground truth is presented in Fig. 8 and Fig. 9, showing detections given by the A-C Guard detector and by the A-C DF-map detector. Target ground truth is marked with plus signs while target detection is marked with rectangular dots. It is observed that target detections match with their ground truth. Despite the fact that the signal processing load of the A-C Guard is only 6 % that of the A-C DF-map, it is evident that those two sequential detectors have the same detection performance, in the sense that they give almost the same number of detection points for each of the four targets B717 and DA40(1,2,3).

VII. Discussion and Future Work

It is reported in the companion paper [2] that the A-C DF-map detector has approximately 5 dB detection gain compared to the one-step detector (which applies a sliding-window CA detector on the DF-map). It is evident in Sections V and VI that the A-C Guard detector has a detection performance which is comparable to that of the A-C DF-map detector. Therefore, it can be seen that sequential detectors can perform much better than a conventional one-step detector. In this application, the gain of the A-C Guard detector comes from two aspects.

Firstly, in the alert step, the (broadest) Guard beam replaces all 300 beams which are designed to cover the whole surveillance space. Therefore, detection on 300 RD-maps now reduces to detection in only one (Guard) RD-map. The reduction in the number of threshold tests allows the false alarm to be set at a very high value (F_1 = 0.05) to detect targets of small SNR, compensating for the reduction in SNR when detection is performed on the Guard RD-map.

Secondly, in the confirm step, a target's SNR is improved by beamforming in the direction of the suspected target being revisited. Such improvement in a target's SNR allows the overall false alarm to be set at a lower value ($F=10^{-6}$). This means that a high detection threshold can be set in the confirm step to eliminate a lot of alert false alarms. It is found that the interference in the RD-maps obtained by beamforming in the AoA of the suspected target has an exponential distribution. Therefore, the Pd in the confirm step is the Pd of the optimal CA-CFAR detector performed on exponentially distributed background. Referring to (7), the product of the alert and confirm Pds is at best equal to the confirm Pd. Provided that the alert Pd is high (which can be achieved with a high false alarm rate F_1), the product of the two Pds will approach the confirm Pd. This explains why the overall Pd of the A-C Guard detector is very close to that of the optimal detector.

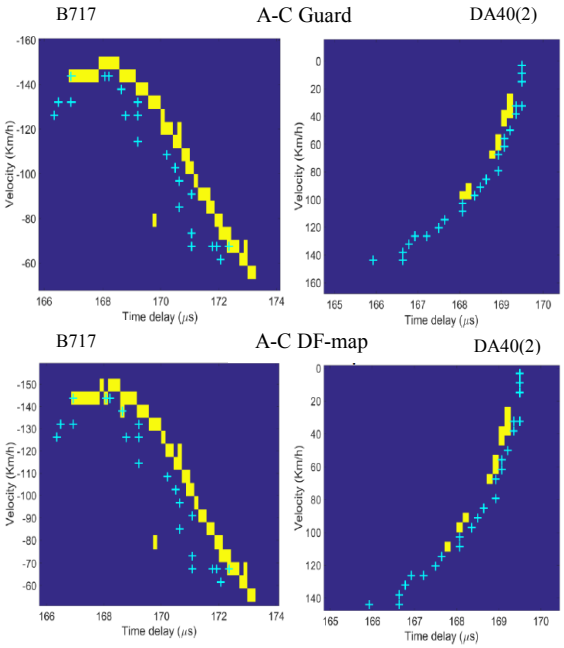

Fig.8 Detection of targets B171 and DA40(2) versus ground truth. Rectangular dots: detections; plus sign: ground truth.

In Fig. 2 (bottom), the CDF of a range profile in the Guard RD-map is shown on Weibull paper [10]. On this transformed plot, the empirical CDF of a data set having exponential distribution will align along a straight line. It is evident that the interference background of the Guard RD-map is not exponentially distributed since the observed CDF does not align on a straight line. A sliding-window CA detector only gives CFAR characteristic if the distribution of interference background is exponential [8]. The alert step of the Guard RD-map detector then does not have the CFAR characteristic.

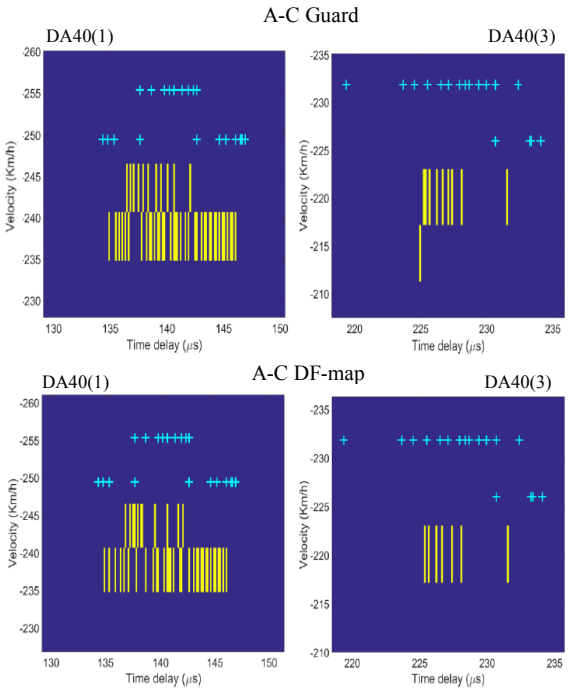

Fig. 9 Detection of targets DA40(1) and DA40(3) versus ground truth. Rectangular dots: detections; plus sign: ground truth.

In this application, cascading a non-CFAR detector (alert step) to a CFAR detector (confirm step) gives a non-CFAR detector. However, it is found that the overall behavior of the A-C Guard detector tends toward that of the CFAR detector of the confirm step, in the sense that:

- The combined alert-confirm false alarm rate fluctuates 1.6 times around the nominal value (the observed false alarm behavior of the Guard RD-map detector is similar to that of the A-C DF-map detector which is reported in the companion paper [2]).
- The detection curve of the combined alert-confirm detector is very close to that of the CA-CFAR detector applied on exponentially distributed background, if the alert false alarm rate is set high enough.
- The threshold multiplier of the confirm test can be approximated using the close-form formula of the CA-CFAR detector operating on exponentially distributed background.

One way to give the alert step CFAR characteristic is to perform alert detection on each of the M elementary RD-maps $|\mathbf{X}_1|^2,\ldots,|\mathbf{X}_M|^2$ in (1) and then apply the combination rule m-of-M ($m \le M$). That means a target is suspected if the alert test is passed in at least m elementary RD-maps.

The use of the Guard channel beam is a special case in which only one alert beam is formed to cover the full 360° surveillance space. A number of alert beams, each with a narrower azimuth beamwidth, can also be used. A balance between performance improvement and processing time using a number of alert beams is worthy for investigation.

CONCLUSION

Two sequential detectors are proposed for multi-channel PCL radar detection, namely, the A-C DF-map detector and the A-C Guard detector. The former is presented in a companion paper (Part 1), while the latter is presented in this paper (Part 2). The A-C Guard detector uses the Guard beam for detection in the alert step. Its detection performance is analysed using Monte-Carlo simulation and experimental data, while a real detection scenario is employed to verify its performance. Closed-form formulas are derived to compute the sequential detection threshold multipliers given the required false alarm rates. The signal processing load of the A-C Guard detector is only 6 % of that of the A-C DF-map detector, while Monte-Carlo analysis and experimental results from a real target scenario show that the A-C Guard detector performs comparably with the A-C DF-map detector.

ACKNOWLEDGEMENT

All experimental data files analysed in this paper were obtained thanks to the support of the DST Group's PCL team. The readability of the paper is improved thanks to inputs from Mr Robert Young and Dr Brett Haywood.

APPENDIX

For an M-channel ring array PCL system, the DF-map is formed as follows. Assume that the surveillance space can be covered by K beams steering at K resolution angles $\theta_1,\ldots, \theta_K$. Using M elementary RD-maps at M channels, one RD-map is formed at each of those K AoAs, giving K directional RD-maps $\mathbf{X}_{\theta 1},\ldots, \mathbf{X}_{\theta K}$. The DF-map, denoted as $\mathbf{Y}$, is formed as:

$$\mathbf{Y}(m,n) = max\ [|\mathbf{X}_{\theta 1}(m,n)|^2,\ldots, |\mathbf{X}_{\theta K}(m,n)|^2] \qquad (8)$$

where (m,n) denotes (Doppler index, range index). The angle θ_t where the maximum is obtained is hypothesised as target's AoA at cell (m,n) [5].

REFERENCES

[1] W.L. Melvin and J.A. Caheer, Principles of Modern Radar: Advanced Techniques, Chapter 17, SciTech Publishing, 2014, USA.

[2] T.V. Cao, "Sequential detection for passive radar, Part 1: the A-C DF-map detector", IEEE Radar Conference 2018, Brisbane, Australia.

[3] D.K. Barton, Radar System Analysis and Modeling, Artech House 2005.

[4] G. Morris and L. Harkness, Airborne Pulse Doppler Radar, Artech House, 1996, USA.

[5] J. Palmer, "A signal processing scheme for a multichannel passive radar system", ICASSP 2015, Brisbane, pp. 5575-5579.

[6] A.Z Elsherbeni and M. Inman, Antenna Design and Visualization Using Matlab, SciTech Publishing, 2006.

[7] W. Bürger and U. Nickel, "Space-time adaptive detection for airborne multifunction radar", IEEE radar conference 2008, pp1-5.

[8] P.P. Gandhi and S.A. Kassam, "Analysis of CFAR processors in nonhomogeneous background", IEEE Transactions on Aerospace & Electronic Systems, 1988, 24, (4), pp427-445.

[9] A. De Maio (Editor), Modern Radar Detection Theory, Chapter 4, Scitech Publishing, 2016.

[10] M. Sekine and Y. Mao, Weibull Radar Clutter, Peter Peregrinus, 1999.